THEORETICAL BIO-SIGNIFICANCE EVALUATION OF QUINAZOLINE ANALOGUES

ABSTRACT

Structure of nine quinazoline derivatives were optimized using density functional theory method in order to probe into the bioactive conformations of the compound. The obtained descriptors which described the anti-neuroepithelioma activity of the compounds were selected and used to develop a model using partial least square method. The developed model replicated the experimental IC_{50} indicative of the predicting power of the model. In addition, ligand-receptor interactions are reported and 2-((E)-2-(4-Bromo-phenyl)-vinyl)-3H-quinazolin-4-one (**A_4**) showed the greatest affinity to bind on the active site of human neuroepithelioma cell line.

Keywords: QSAR, DFT, quinazoline analogues, docking, neuroepithelioma cell line.

1.0 INTRODUCTION

Several natural and synthetic quinazoline based products as antimicrobial agents have been successfully developed over the last four decades [1,2]. Quinazoline, a heterocyclic compound with molecular formula, $C_8H_6N_2$, has a double-ring structure consisting of a benzene ring fused with pyrimidine ring, and exists as yellow crystals [3,4]. Quinazoline and its derivatives have shown various biological activities as antidepressant anti-inflammatory, antimalarial, anticancer, antifungal, antimicrobial, antiviral, anti-tubercular, anti-protozoan, anticonvulsant [5-8].

Quantitative Structural Activity Relationship (QSAR) is a numerical model that link series of molecular parameters of a molecules to its bioactivity [9]. In the discovery, design and development of drug-like molecules, quantitative structural activity relationship has

gained a vast usefulness which has drawn several researchers to studying bioactivity of compounds via QSAR [10].

The use of docking as a means of studying the connectivity that is existing between ligands and enzyme (receptor) has been extensively recognized. It shows the basic ways that drug-like compounds used in preventing targeted binding site [11,12].

Bio-significance of molecular compounds is determined by the structure and the electronic properties of the molecules. Thus, in this work, the optimised structure and electronic properties of 2-((E)-Styryl)-3H-quinazolin-4-one (**A_1**), 2-((E)-2-(2-Methoxy-phenyl)-vinyl)-3H-quinazolin-4-One (**A_2**), 2-((E)-2-(3-Methoxy-phenyl)-vinyl)-3H-quinazolin-4-one (**A_3**), 2-((E)-2-(4-Bromo-phenyl)-vinyl)-3H-quinazolin-4-one (**A_4**), 4-Chloro-2-((E)-styryl)-quinazoline (**B_1**), 4-Chloro-2-((E)-2-(2-methoxy-phenyl)-vinyl)-quinazoline (**B_2**), 4-Chloro-2-((E)-2-(3-methoxy-phenyl)-vinyl)-quinazoline (**B_3**), 4-Chloro-2-((E)-2-(4-methoxy-phenyl)-vinyl)-quinazoline (**B_4**) and 4-Chloro-2-((E)-2-(2,4-dimethoxy-phenyl)-vinyl)-quinazoline (**B_5**) were computed using quantum chemical method with a view to theoretically investigate the anti-human neuroepithelioma activity of the compounds through the development of a quantitative structural activity relationship, QSAR and molecular docking study. This set of nine quinazoline derivatives have been experimentally shown to have expressive bioactivity against human neuroepithelioma [13].

2.0 MATERIALS AND METHODS

2.1 *Optimization*

The studied compounds (Figure 1) were optimized using density functional theory via 6-31G* basis set. The density functional theory method used in this work was done with B3LYP density functionals which include Becke's gradient exchange [14] and Lee, Yang and Parr correlation [15]. The accuracy of density functional theory calculations is based on the selected basis set. Among the calculated descriptors are the highest occupied molecular

orbital (E_{HOMO}) energy, lowest unoccupied molecular orbital (E_{LUMO}) energy, dipole moment, chemical potential, chemical hardness, etc. The quantum chemical calculations were done using Spartan '14 software by wavefunction Inc [16].

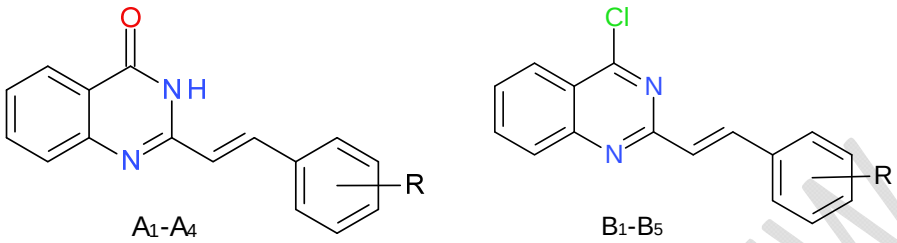

A_1: H, A_2: 2-OMe, A_3: 3-OMe, A_4: 4-Br, B_1: H, B_2: 2-OMe, B_3: 3-OMe, B_4: 4-OMe, B_5: 2, 4-OMe.

Figure 1: Schematic structures of the studied Quinazolines

2.2 Descriptor selection and QSAR model development

The study of quantitative structure activity relationship (QSAR) require the use of appropriate molecular descriptors (with high simplicity and high predicting power) from the entire calculated descriptors [17,18]. Therefore, QSAR model was developed via partial least square method and this was used to calculate the predicted bioactivity. The software used for partial least square method was XLSTAT 2018 [19].

2.3 *Quality and Validation of QSAR Model*

The evaluation of the quality and validation of developed QSAR model were done by considering cross validation (Cv.R^2) and adjusted R^2 $\left(R^2_{adj}\right)$ [Equation 1 and 2].

$$CV.R^2 = 1 - \frac{\sum(Y_{obs} - Y_{cal})^2}{\sum(Y_{obs} - \bar{Y}_{obs})^2} \text{----------(1)}$$

The adjusted R^2 could be calculated using equation (2)

$$R^2_a = \frac{(N-I)\times R^2 - P}{N-1-P} \text{----------(2)}$$

The developed quantitative structural activity relationship model could be considered prognostic, if $C_v.R^2 > 0.5$ and $R^2_{adj} > 0.6$ [20-22].

2.4 *Molecular docking studies*

Molecular docking studies were performed by using the following softwares; Discovery Studio 4.1, Autodock tools 1.5.6, Autodock vina 1.1.2, and pymol 1.7.4.4. The receptor used in this work was obtained from protein data bank and adjusted for docking purpose. For the purpose of accuracy in docking, the residues (water molecules and crystallized drug-like molecules) were removed from the protein (**4bjx**) [23]. The treated receptor was subjected to autodock tool 1.5.6 for location of binding site and development of a grid box (centre grid box: x:-3.872; y:-4.818; z:-18.982) to cover the neuroepithelioma cell line binding site. Autodock vina software was employed to simulate the ligand into the active site of the receptor (protein) in order to calculate the binding energy of the ligand-receptor complexes. Also, inhibition constant was calculated using equation 3.

$$K_i = e^{\frac{-\Delta G}{RT}} \text{ ---------- (3)}$$

3.0. *Results and Discussion*

3.1 Electronic Descriptors and QSAR Studies

The calculated descriptors include E_{HOMO}, E_{LUMO}, dipole moment (DM), Log P, molecular weight (MW), polar surface area (PSA), polarizability and ovality (Table 1).

Table 1: The calculated molecular descriptors obtained for quinazoline derivatives

Comp	HOMO (eV)	LUMO (eV)	BG (eV)	DM (Debye)	LOGP	MW	OVALITY	PSA (Å^2)	HBD	HBA	POL	IC_{50}
A_1	-6.04	-1.70	4.34	4.12	3.39	248.285	1.40	32.085	0	2	61.55	1.39
A_2	-6.02	-1.74	4.28	4.82	3.26	278.311	1.42	39.584	0	4	63.56	2.88
A_3	-5.98	-1.73	4.25	5.71	3.26	278.311	1.46	39.100	0	3	63.77	5.13
A_4	-6.05	-1.80	4.25	2.16	4.22	327.181	1.44	32.079	0	2	63.04	2.85
B_1	-6.16	-2.28	3.88	3.10	4.83	266.731	1.41	13.636	0	3	62.18	4.96
B_2	-5.91	-2.37	3.54	4.05	4.71	297.757	1.46	20.169	0	3	64.41	0.58
B_3	-5.96	-2.41	3.55	3.72	4.71	296.757	1.46	20.935	0	8	64.40	5.28
B_4	-5.78	-2.37	3.41	4.35	4.71	296.757	1.46	20.938	0	2	64.43	4.34
B_5	-5.72	-2.35	3.37	2.93	4.58	326.783	1.51	26.775	0	3	66.64	1.75

The calculated descriptors were used as independent variables and the experimental IC_{50} (Table 2), served as dependent variables in the development of QSAR model using multiple linear regression. This was used to select the molecular parameters that perfectly describe anticancer activity of quinazolines. The developed QSAR model (Equation 4) was used to predict the bioactivity of the studied compounds (Table 2). The calculated squared correlation coefficient (R^2) (0.947) and the adjusted R^2 (0.894) revealed the predicting power and quality of the model developed as shown in Table 3. The model reproduced the observed IC_{50} as depicted by the residual values (Observed IC_{50} – Predicted IC_{50}) (Table 2).

IC_{50} = -597.570 -10.5191(LOGP) + 21.8795(HET) - 59.9882(LUMO) -891.799(N1) ----------(**4**)

Table 2: Observed IC_{50} and Predicted IC_{50}

	Observed IC_{50}	Predicted IC_{50}	Residual
A_1	1.39	1.47	-0.08
A_2	2.88	3.38	-0.50
A_3	5.13	4.61	0.52
A_4	2.85	2.76	0.09
B_5	4.96	4.99	-0.03
B_6	0.58	0.57	0.01
B_7	5.28	4.75	0.53
B_8	4.34	5.03	-0.69
B_9	1.75	1.61	0.14

Table 3: Statistical parameters for developed QSAR model

N	p	R^2	R^2_{adj}	$CV.R^2$
9	4	0.947	0.894	0.984

This developed QSAR model as shown in equation 4 shows a positive input of Heteroatom. However, log P, LUMO and Charge on Nitrogen (1) (N1) contributed negatively to the bioactivity and this was suggesting that, as log P, LUMO and Charge on Nitrogen (1) (N1) decreases, biological activity of Quinazoline derivatives increases and vice-versa for Heteroatom. The QSAR model showed that the anticancer activity of the compounds was directly linked to these molecular parameters. Figure 2 demonstrates the quality of the developed QSAR while as shown in Figure 3, the residual values were observed on both positive and negative sides of the graph and this indicated that there was no systemic inaccuracy in the developed QSAR model.

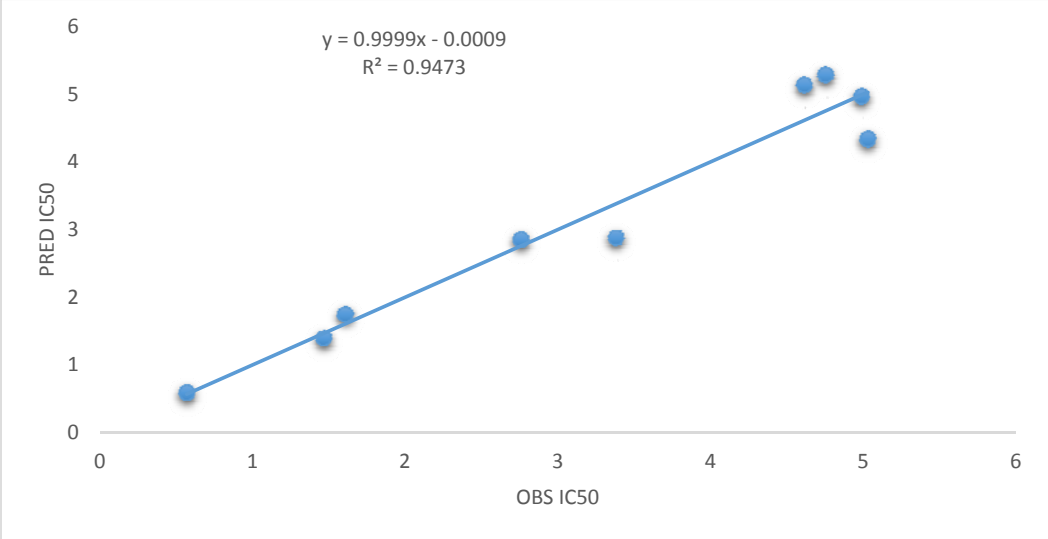

Figure 2: Plot of predicted IC_{50} against observed IC_{50}

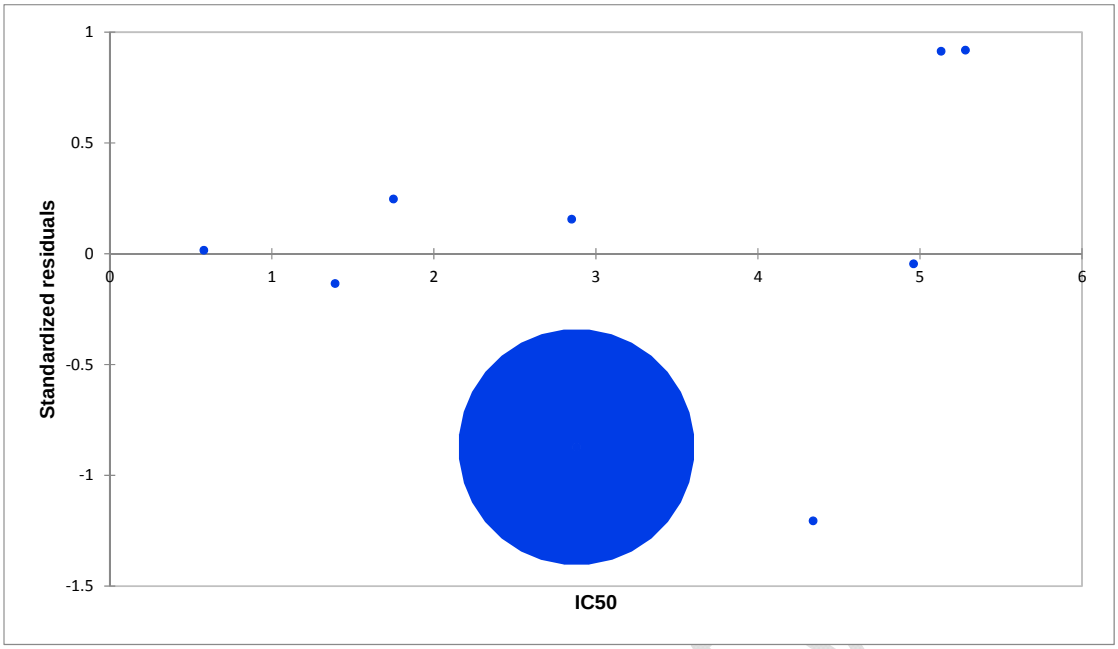

Figure 3: Plot of residual values against observed IC_{50}

4.0 *Docking Studies*

The study of molecular docking was executed in this research in order to comprehend the binding mode of drug-like molecule against the receptor (**4bjx**). First and foremost, Ramachandran plot was used to evaluate the orientation and conformation of human neuroepithelioma cell line (**PDB ID: 4bjx)**, and it was discovered that almost all the residue in the studied receptor (i.e. 99.2% of the residues) was found in a favoured region and the entire residues (i.e. 100.0% of the residues) were in allowed regions. More so, there were no outliers as shown in Figure 4. Thus, the receptor used in this work was stable and of a good quality. As shown in Table 4, the dock scores for ligand-receptor complexes ranged from -8.2 to -7.6 kcal/mol and it was discovered that $\mathbf{A_4}$ had the highest possibility to inhibit human neuroepithelioma cell. The residues involve in the interaction between studied compounds (A_1-B_5) and **4bjx** were VAL-87, CYS-136, LEU-92, TRP-81, PRO-82 for $\mathbf{A_1}$, LEU-92, TRP-81, VAL-87, ASN-140, PRO-82, CYS-136, ILE-146 for $\mathbf{A_2}$, ASN140, CYS-136, PRO82, GLN-85, LEU-92, LYS-91, ILE-146, VAL-87 for $\mathbf{A_3}$, ASN140 and PRO82 for A4,

CYS-136, VAL-87, LEU-92, PRO-82, ILE-146, TRP-81 for B1, VAL-87, CYS-136, LEU-92, PRO-82, TRP-81 for **B_2**, MET-132, MET-105, PRO-82, TRP-81, VAL-87, ILE-146, CYS-136, LEU-92 for **B_3**, LEU-92, VAL-87, CYS-136, ILE-146, MET-105, TRP-81 for **B_4** and CYS-136, ILE-146, VAL-87, GLN-85, LEU-92, TRP-81, TYR-97, LEU-94, TYR-139 for **B_5.** The ligand and receptor complex displayed in Figure 5 showing the residue that was involved in the interaction together with hydrogen bonds for A_4.

Also, Lipinski's rule of five was observed for the compounds used in this work and all the studied compounds proved to be drug-like compounds. As shown in Table 1, the molecular weight value were ≤ 500, Hydrogen bond acceptor were ≤10, Hydrogen bond donor were less than ≤5 and calculated logP value were also ≤ 5.

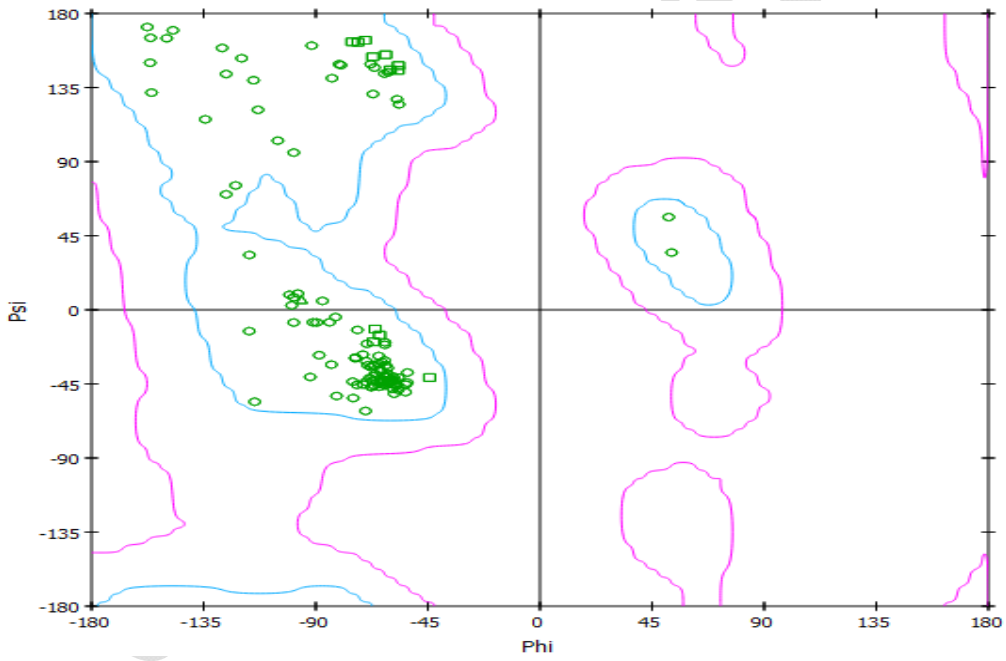

Figure 4: Ramachandran plot for human neuroepithelioma cell line (**PDB ID: 4bjx)** [23]

Table 4: Ligand-receptor dock score of quinazoline derivatives with 4bjx.

Compound	Affinity (kcal/mol)	K_i (µM)	Interacting Residues
A_1	-8.1	8.72×10^5	VAL-87, CYS-136, LEU-92, TRP-81, PRO-82
A_2	-8.0	7.37×10^5	LEU-92, TRP-81, VAL-87, ASN-140, PRO-82, CYS-136,

			ILE-146
A_3	-8.1	8.72×10^5	ASN140, CYS-136, PRO82, GLN-85, LEU-92, LYS-91, ILE-146, VAL-87
A_4	-8.2	1.03×10^6	ASN140 and PRO82
B_1	-8.1	8.72×10^5	CYS-136, VAL-87, LEU-92, PRO-82, ILE-146, TRP-81
B_2	-8.1	8.72×10^5	VAL-87, CYS-136, LEU-92, PRO-82, TRP-81
B_3	-7.8	5.25×10^5	MET-132, MET-105, PRO-82, TRP-81, VAL-87, ILE-146, CYS-136, LEU-92
B_4	-7.7	4.44×10^5	LEU-92, VAL-87, CYS-136, ILE-146, MET-105, TRP-81
B_5	-7.6	3.75×10^5	CYS-136, ILE-146, VAL-87, GLN-85, LEU-92, TRP-81, TYR-97, LEU-94, TYR-139

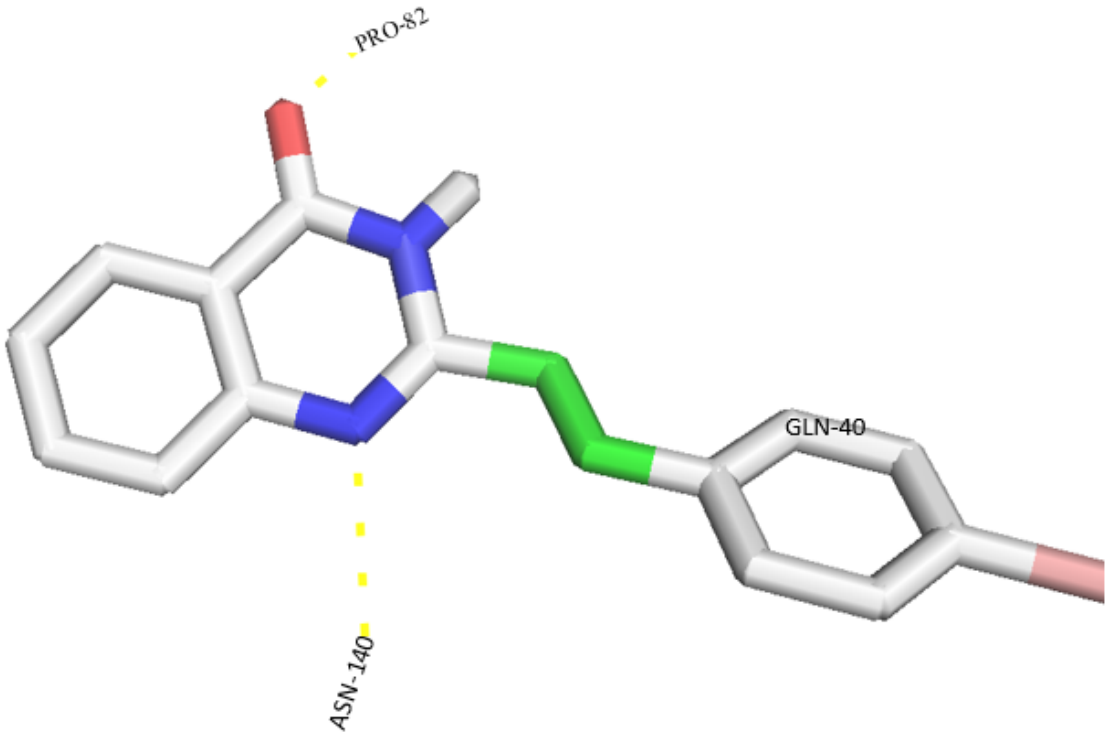

Figure 5: Interactions of **A_4** with the residue in the active gouge of human neuroepithelioma cell line (**4bjx**).

Conclusion

The anti-human neuroepithelioma activity of quinazoline analogues was observed using theoretical approach. In this study, density functional theory was use to optimized the molecular compounds and the descriptors obtained were used for QSAR analysis using partial least square method. The descriptors, E_{HOMO}, E_{LUMO}, Log P, ovality, PSA, and molecular weight were implicated in the anti-human neuroepithelioma activity of quinazoline derivatives and the developed QSAR model replicated the experimental IC_{50}. Also, 2-((E)-2-(4-Bromo-phenyl)-vinyl)-3H-quinazolin-4-one (**A_4**) inhibited the 4bjx most as revealed by the affinity and the inhibition constant (K_i).

Ethical approval and consent are not applicable

REFERENCE

[1]. Carlos MMG and Vladimir VK. Recent Developments on Antimicrobial Quinoline Chemistry, Microbial pathogens and strategies for combating them: science, technology and education (A. Méndez-Vilas, Ed.), 2013.

[2] Majumdar KC and Chattopadhyay SK. Heterocycles in Natural Product Synthesis. Wiley-VCH, 1-658, 2011.

[3] Connolly DJ, Cusack D, O'Sullivan TP, and Guiry PJ. Synthesis of quinazolinones and quinazolines. Tetrahedron. 2005; 61(43): 10153–10202.

[4] Abida PN and Arpanarana M. An updated review: newer quinazoline derivatives under clinical trial. International Journal of Pharmaceutical & Biological Archive. 2011; 2(6):1651–1657.

[5]. El-Messery SM, Hassan GS, Al-Omary FAM, El-Subbagh HI. Substituted thiazoles VI. Synthesis and antitumor activity of new 2-acetamido- and 2 or 3-propanamido-thiazole analogues. Eur. J. Med. Chem. 2012; 54:615–625.

[6]. Berest GG, Voskoboynik OY, Kovalenko SI et al. Synthesis and biological activity of novel N-cycloalkyl-(cycloalkylaryl)-2-[(3-R-2-oxo-2H-[1, 2, 4] triazino [2, 3-c] quinazoline-6-yl) thio] acetamides. Eur. J. Med. Chem. 2011;46:6066–6074.

[7]. Hu J, Zhang Y, Dong L, et al. Design, synthesis, and biological evaluation of novel quinazoline derivatives as anti-inflammatory agents against lipopolysaccharide-induced acute lung injury in rats. Chem. Biol. Drug Des. 2015;85:672–684.

[8]. Ammerdorffer A, Stojanov M, Greub G, et al. Chlamydia trachomatis and chlamydia-like bacteria: new enemies of human pregnancies. Curr. Opin. Infect. Dis. 2017;30:289–296.

[9]. Hansch C. A quantitative approach to biochemical structure-activity relationships. Acc of Chem Res. 1969;2:232-239.

[10]. Ramsden CA. Quantitative Drug Design of comprehensive Medicinal Chemistry, Oxford. 1990; 4.

[11]. Cherfils J, Janin J. Protein docking algorithms: simulating molecular recognition. Curr. Opin. Struct. Biol. 1993; 3: 265-269.

[12]. Kuntz ID, Meng EC, Shoichet BK. Structure-Based Molecular Design. Acc. Chem. Res. 1994;27: 117-123.

[13]. Anna M-W, Danuta SK, Robert M, Jacek F, Agnieszka S, Katarzyna S, Knas M, Sishir KK, Zaklina K, Josef J, Alicja R, Joanna, R-W. Investigating the anti-proliferative activity of styrylazanaphthalenes and azanaphthalenediones. Bioorganic & Medicinal Chem. 2010;18:2664–2671.

[14]. Becke AD. Density-functional thermochemistry. III. The role of exact exchange. J. Chem. Phys. 1993;98:5648-5652.

[15]. Lee C, Yang W, Parr RG. Development of the Colle-Salvetti correlation-energy formula into a functional of the electron density.Condens. Matter. Phys Rev B. 1988;37(2):785-9. [DOI: 10.1103/PhysRevB.37.785].

[16]. Spartan 14, Wavefunction, INC, Irvine CA 92612, USA

[17] Leardi R, Boggia R, Terrile M. Genetic algorithms as a strategy for feature selection. J Chemomet. 1992;6:267–281.

[18]. Pourbasheer E, Riahi S, Ganjali MR, Norouzi P. Application of genetic algorithm support vector machine, (GA–SVM) for prediction of BK-channels activity. Eur. J of Med Chem. 2009;44: 5023–5028.

[19]. www.xlstat.com

[20]. Golbraikh A, Tropsha A. Beware of q2! J Mol Graph Model. 2002; 20:269–276.

[21]. Marrero PY, Castillo GJA, Torrens F, Romero ZV and Castro EA. Atom, atom-type, and total linear indices of the molecular pseudograph's atom adjacency matrix": application to QSPR/QSAR studies of organic compounds. Molecules. 2004;9(12):1100–1123.

[22]. Oyebamiji AK and Semire B. DFT-QSAR and Docking Studies of 2-[5-(aryloxymethyl)-1,3,4-oxadiazol-2-ylsulfanyl] acetic acids Derivatives against *Bacillus subtilis.* Der Pharma Chemica. 2018; 10(3):135-139.

[23]. Wyce A, Ganji G, Smitheman KN, Chung C-W, Korenchuk S et al. BET Inhibition Silences Expression of *MYCN* and *BCL2* and Induces Cytotoxicity in Neuroblastoma Tumor Models. PLoS ONE. 2013;8(8), e72967. doi:10.1371/journal.pone.0072967.